An assessment of dose-dependent UV-B sensitivity in *Eclipta alba*: Biochemical traits, antioxidative properties, and wedelolactone yield

Kshama Rai[1] · Shashi Bhushan Agrawal[1]

Abstract

The UV-B-induced signals play a crucial role in improving the analeptic values of medicinally important plants. *Eclipta alba* L. (Hassak), commonly known as False Daisy, holds supreme stature with its pharmaceutical association in treating various ailments, particularly in Ayurvedic medicine. The present study aimed to evaluate the response of *E. alba* plants exposed to ambient (AT) and two different supplemental UV-B doses (eUV-B, ambient ± 7.2 kJ m^{-2} day^{-1}), i.e., intermittent (IT) and continuous (CT) UV-B treatment for 130 and 240 h respectively. Antioxidative activities and medicinally important compounds (wedelolactone) were measured in different plants' parts at three growth stages. Under both the eUV-B treatments, the photosynthetic pigments were adversely affected (along with reductions in protein content) with a concomitant increase in secondary metabolites. Substantial variations in enzymatic antioxidants and non-enzymatic compounds showed the adaptive resilience strategies of plants against eUV-B. The wedelolactone content increased in leaves but compromised in stem and roots under IT. The results concluded that IT UV-B exposure led to the improvement of plant growth and the yield of wedelolactone compared to CT, suggesting its ameliorative role in improving the test plant's medicinal value.

Keywords *Eclipta alba* · Reactive oxygen species · Enzymatic antioxidants · Non-enzymatic antioxidants · UV-B

Introduction

The harmful ultraviolet-B (UV-B) penetration and its intensity depend on several factors, namely temporal, geographic, atmospheric, and climatic conditions, and can modulate the effects of UV-B on plants. Terrestrial plants being sessile inevitably encounter harsh solar radiation, including UV-B radiation. UV-B, along with other biotic and abiotic stresses, plays an important role in disordering the plants' photomorphogenic changes. Excessive UV-B exposure displays attenuated plant metabolic responses and related feedback (Höll et al. 2019). Supplemental UV-B exposure is known to mediate several morphological and physiological changes (Kataria et al. 2014; Takshak and Agrawal 2018; Rai and Agrawal 2020) as well as increased biosynthesis and accumulation of UV absorbing secondary metabolites and antioxidants (Mosadegh et al. 2018; Takshak and Agrawal 2018). Several studies revealed that exposure to lower or intermittent/pulsed levels of UV-B radiation plays hormetic effects (Höll et al. 2019; Kumari et al. 2009), while excessive, continuous UV-B exposure induces harmful and damaging effects on the plants (Rai and Agrawal 2020). To withstand such harsh and stressful conditions, plants induce the biosynthesis and accumulation of UV-protective compounds such as phenolic compounds, flavonoids, alkaloids, and terpenes, which are known to mitigate the UV-B damage by their accumulation at the leaf surfaces.

Besides the damaging nature, increased secondary metabolites' properties due to UV-B could be implicated as medicinally important drug extraction to protect plants and animals (Takshak and Agrawal 2019). Modifications in the UV-B dose, intensity, and duration could increase the biosynthesis of stress-induced defensive compounds (Höll et al. 2019), which is thereafter used in harvesting

✉ Shashi Bhushan Agrawal
   sbagrawal56@gmail.com

   Kshama Rai
   kshamarai9@gmail.com

[1] Laboratory of Air Pollution and Global Climate Change, Department of Botany, Institute of Science, Banaras Hindu University, Varanasi 221005, India

the medicinally valuable compounds. Despite all the protective adaptation and stress-defense strategies, the overall plant's performances are often accompanied by high metabolic costs and developmental penalties. To understand these cost-benefit relationships among the abiotic stress, i.e., UV-B, and plants, several studies have been done focusing mainly on the single acute short-term or long chronic UV-B exposures (Kumari et al. 2009; Tripathi et al. 2011; Takshak and Agrawal 2014a, b, 2015, 2018; Sebastian et al. 2018). Nevertheless, plants encounter fluctuations in the prevailing stress conditions and little or long recovery periods in natural conditions. The response of plants against such dynamically moving ecologically driven field environments is hitherto less explored.

To fill this lacuna, the present study was focused on ambient (control) versus continuous (CT) and intermittent (IT) UV-B exposure at three growth stages to explore the understandings of the dynamic responses of *Eclipta alba* L. (Hassak) plants. The wildly grown *E. alba* plant was the choice for this study, as it is medicinally important and is widely used in Ayurvedic treatments of liver cirrhosis, hepatitis, and baldness. Various studies revealed that wedelolactone is the primary medicinal compound of the test plant. However, the plant part and growth stages at which wedelolactone concentration is highest for commercial extraction of this compound are still debatable. Wedelolactone (7-methoxy-5,11,12-trihydroxy-coumestan) is a coumestans compound derived from coumarin derivatives used to protect the liver from damage and inflammation, septic shocks, and venom poisoning (Rai and Agrawal 2020; Luo et al. 2018).

The study was hypothesized to find whether IT or CT UV-B exposure modulates the test plant's biochemical defense strategies vis-a-vis medicinally important wedelolactone biosynthesis and accumulation in different plant parts and at different growth stages as compared to ambient UV-B exposures. To fulfill the hypothesis, the present study estimates the response of *E. alba* against ambient, IT, and CT UV-B treatments through the assessment of the following objectives: (1) to evaluate the changes in photosynthetic pigments, primary and secondary metabolites; (2) to assess the antioxidative and reactive oxygen species production; and (3) to determine the amount of medicinal compound wedelolactone found in different parts of the test plant at different developmental stages concerning IT and CT UV-B exposures.

Materials and methods

Experimental site, plant material, treatments, plant sampling, and biochemical analyses

The present field-based study was conducted at the Botanical Garden (25° 16′ 4.1″ N and 82° 59′ 20.9″ E), Banaras Hindu University, Varanasi, India. For the experimental investigations, *Eclipta alba* L. (Hassk), False Daisy (or *Bhringaraaj*), belonging to the family Asteraceae, was sown under natural field conditions. The seeds were obtained from the Botanical Garden, Banaras Hindu University, which took a week for germination. The UV-B treatments were given 30 days after germination (DAG) of *E. alba* seeds.

The seeds were sown in the experimental plots of 1×1 m^2 dimension. The study was based on nine plots: three control plots (AT) (plants, receiving ambient UV-B), three plots for IT (plants receiving ambient + 7.2 kJ m^{-2} day^{-1} elevated UV-B on alternate days), and three for CT (plants receiving ambient + elevated UV-B daily) up to the end of the study, i.e., day 180. The elevated UV-B (eUV-B) dose was provided artificially to the plants for 3 h (11:00 to 14:00) over the mid of the total photoperiod using Q panel UV-B 313, 40-W fluorescent lamps (Q panel Inc. Cleveland OH, USA). The plants exposed with IT and CT received 130 and 240 h ambient+7.2 kJ m^{-2} day^{-1} dose throughout the investigation period, respectively. The distance between lamps and plants was adjusted at equal distances (45 cm from the tip of the test plant) on adjustable steel frames perpendicular to the plant and was covered with cellulose diacetate filters of 0.13-mm thickness. The entire experimental setup was scheduled for replacement on weekly basis in order to sustain the evenness in optical properties of the filters.

From each plot, plants were randomly sampled (five replications for each treatment for biochemical parameters) and assessed for photosynthetic pigments, secondary metabolites accumulation, reactive oxygen species (ROS) production, and the antioxidative activities of non-enzymatic and enzymatic compounds, along with some phenylpropanoid pathway-related enzymes and wedelolactone content in different parts of the test plant.

Meteorological and UV-B monitoring

The daily monitoring of ambient photosynthetic active radiation (PAR) and UV-B radiation was done by using PMA2100 Solar Radiometer (100 East Glenside Avenue, Glenside, PA 19038, USA). Meteorological variables such as daily temperature (maximum, minimum, °C), relative humidity (%), cloud condition (%), and rainfall (mm) during the experiment were recorded from the unit of the Indian Meteorological Department, Banaras Hindu University. The seasonal mean maximum and minimum temperatures were 31.5 and 22.7 °C, respectively. However, average PAR and clouds were 956 μmol m^{-2} s^{-1} and 25.2% during the study period, respectively (Table 1). The seasonal mean of relative humidity and rainfall at the experimental period were 55.2% and 355 mm, respectively (Table 1).

Table 1 UV-B treatment and weather conditions during the experimental period (July 18–Dec 18)

Parameters	Temperature (°C)		RH (%)	Cloud (%)	PAR (μmol m^{-2} s^{-1})	Ambient UV-B (kJ m^{-2} day^{-1})
	Maximum	Minimum				
Seasonal mean	31.5±0.26	22.7±0.4	55.2 ±1.1	25.2±1.6	956±16	15.9±1.4
Treatments	**AT**	**IT**		**CT**	**Total rainfall (mm)**	
Seasonal cumulative values	2385.26	2697.02		2961.26	355.7	

AT ambient UV-B treatment, *IT* intermittent UV-B treatment, *CT* continuous UV-B treatment, *RH* relative humidity, *PAR* photosynthetic active radiation

Photosynthetic pigment content

Chlorophyll *a* and chlorophyll *b* were determined by following the method discussed by Takshak and Agrawal (2018), and absorbance was taken at 645 and 663 nm for chlorophyll *a* and chlorophyll *b* using a double-beam spectrophotometer (Model-2203, Systronics, India).

Reactive oxygen species production and membrane damage

Superoxide radical ($^.O_2^-$) production rate was determined by following the methodology of Elstner and Heupel (1976) using hydroxylamine hydrochloride (10 mM), sulphanilamide (8.5 mM), and α-naphthylamine (3 mM). The absorbance was recorded at 530 nm, and a standard curve was prepared using potassium nitrite to calculate the $^.O_2^-$ radical production.

However, hydrogen peroxide (H_2O_2) content was estimated by the protocol given by Alexieva et al. (2001). The absorbance was recorded at 390 nm, and H_2O_2 content was calculated by the standard graph prepared with the known concentration of H_2O_2.

The extent of membrane damage by ROS-induced lipid peroxidation (LPO) was estimated by the malondialdehyde (MDA) content utilizing thiobarbituric acid (TBA), and the methodology was given by Heath and Packer (1968). The absorbance was recorded at 532 and 600 nm. The MDA content was calculated by the formula used by Takshak and Agrawal (2018).

Metabolites

Protein (mg g^{-1} FW) quantification was done as per Bradford (1976) method. The absorbance was taken at 595 nm and calculated the protein in the sample by using the standard curve of bovine serum albumin (Sigma-Aldrich, Co., USA). Total phenol content was estimated by the method given by Bray and Thorpe (1954) using catechol as the standard compound. The total flavonoid content was evaluated by following the aluminum colorimetric method suggested by Chang et al. (2002) with slight modifications. The absorbance of the florescent green colored solution was recorded and presented at 415 nm. The anthocyanin quantification was done by following Gitelson et al. (2001) protocol, and absorbance was recorded at 535 nm and 650 nm. The difference between the two readings gave the anthocyanin concentration and reported as ΔA g^{-1} fresh weight (Deikman and Hammer 1995). Lignin content was estimated using Syros et al. (2004) (with few modifications). The absorbance of the supernatant was read at 280 nm. Lignin content was expressed as A_{280} g^{-1} fresh weight. For tannins estimation, the method summarized by Khomdram and Singh (2011) was employed (after slight alterations). The optical density was recorded at 700 nm. The calibration curve was prepared using tannic acid and expressed in milligrams per gram of fresh weight.

Non-enzymatic antioxidants

Ascorbic acid content was estimated by the method Keller and Schwager (1977) using 2,6-dichlorophenol indophenol (DCPIP) reduction method, and optical density of the pink colored solution was read at 520 nm (Es). The pink color was then bleached by adding one drop of ascorbic acid (1%), and again its absorbance was recorded at the same wavelength (Et). For blank (Eo), to 1 mL extracting solution, 5 mL DCPIP solutions was added, and absorbance was recorded at the same wavelength. A calibration curve was prepared using known concentrations of ascorbic acid. The method given by Fahey et al. (1978) was used to determine thiol content using Ellman's reagent. The absorbance of the yellow color was measured at 412 nm. Proline content was determined by using the method of (Bates et al. 1973). The absorbance of the chromophore-containing toluene was recorded at 520 nm. The standard curve was prepared with known concentrations of proline.

Enzymatic antioxidative activities

Fresh leaf tissues (200 mg) were pulverized in liquid N_2 for enzyme extraction, and further extraction was done using 5 mL of extracting buffer comprising phosphate buffer (1 M, pH=7.0), ethylene diamine tetra-acetic acid (EDTA),

polyvinyl pyrrolidone (PVP), Triton-X-100, and phenyl methane sulfonyl fluoride (PMSF) at 4 °C. The enzyme activities were assayed using the supernatant.

Superoxide dismutase (SOD) activity was estimated by the 50% NBT reduction method of Beyer and Fridovich (1987) measured at 560 nm. The ascorbic acid–dependent reduction of H_2O_2 at 290 nm given by Hossain and Asada (1984) was used to assay ascorbate peroxidase (APX) activity. The APX activity was calculated by using an extinction coefficient of 2.8 mM^{-1} cm^{-1}. The catalase activity (CAT) was determined by estimating the rate of decrease of H_2O_2 at 240 nm method given by Rubio et al. (2002). The CAT was calculated by using an extinction coefficient of 6.93×10^{-3} mM^{-1} cm^{-1}. The enzyme activity of peroxidase (POD) was estimated by measuring the rate of purpurogallin formed per minute (in μmol) given by Britton and Mehley (1955) and was calculated by using the extinction coefficient of 2.47 mM^{-1} cm^{-1}. The rate of reduction in NADPH absorbance by the oxidation at 340 nm was used to estimate the glutathione reductase (GR) enzyme activity provided by Dalton et al. (1986). The molar extinction coefficient of 6.22 mM^{-1} cm^{-1} was used to calculate GR activity.

Estimation of total ROS potential and enzymatic antioxidative potential

The potential of ROS and enzymatic antioxidants of *E. alba* were calculated by following equations under ambient, intermittent, and continuous UV-B treatments. The ROS and enzymatic potential were calculated similarly to the Response Index by Dai et al. (1994) and cumulative antioxidant potential (CAP) by Takshak and Agrawal (2018).

Total ROS Potential of IT

$$= \sum[(Pi_{IT} - Pi_{AT})/Pi_{AT} \times 100] \tag{1}$$

Total ROS Potential of CT

$$= \sum[(Pi_{CT} - Pi_{AT})/Pi_{AT} \times 100] \tag{2}$$

Enzymatic antioxidative defense potential of IT

$$= \sum[(Pi_{IT} - Pi_{AT})/Pi_{AT} \times 100] \tag{3}$$

Enzymatic antioxidative defense potential of CT

$$= \sum[(Pi_{CT} - Pi_{AT})/Pi_{AT} \times 100] \tag{4}$$

where ROS considers the cumulative changes of LPO, $^{\cdot\cdot}O_2$, and H_2O_2, and antioxidative enzymes consider the cumulative changes of SOD, APX, CAT, POD, and GR under eUV-B treatments compared to ambient. Pi_{AT}, Pi_{IT}, Pi_{CT}: corresponding mean value (Pi) under ambient (AT), intermittent (IT), and continuous (CT) UV-B treatment, respectively.

High-performance liquid chromatography analysis and study

Plant sampling

For the high-performance liquid chromatography (HPLC) analyses of plant samples, the plant parts were categorized into leaves, stem, and root at all three sampling ages (45, 75, and 110 DAG). The concentrations of wedelolactone were recorded in each of these plant parts in triplicate. For this purpose, the protocol of Kumar and Dhanani (2013) was followed with minor modifications.

Sample preparation

The plant parts of *E. alba* were dried in the shade and were finely powdered using an electric grinder for extract preparation. Powdered plant material was extracted with HPLC grade methanol (MeOH) (100 mL × 6) for 24 h at 25 °C. The methanolic extracts were pooled together, filtered, and subjected to centrifugation for 15 min at 6000*g*, concentrated under reduced pressure in rotatory evaporator to obtain the methanolic extract. The supernatant was stored in a 10-mL volumetric flask and adjusted to a final volume with MeOH. Before injection in the HPLC column, the samples were filtered using 0.45-μm nylon membrane filters.

Calibration

One milligram of wedelolactone standards (Sigma-Aldrich) was placed in a volumetric flask and dissolved in MeOH (concentration = 1 mg mL^{-1} stock solution). Five additional calibration levels were prepared by diluting the stock solutions with concentrations ranging from 100 to 20 μg mL^{-1}, over which the detector response was linear (Fig. 6).

Analytical method

Separation of wedelolactone was carried out via HPLC equipped with a photodiode array (PDA) detector (Waters, Milford, MA, USA) having Nova-Pak C18 column (250 × 4.6 mm, 5-μm particle size). The mobile phase consisted of acetonitrile:water:acetic acid in the ratio 95:5:0.04. The column's temperature was kept at 25 °C; the flow rate and sample volume injected were 0.6 ml min^{-1} and 10 μL, respectively. The run time of the samples was 10 min. All separations were monitored at 352 nm. Coumestan derivatives in the samples were identified by running the standards individually following the above methodology.

At 352-nm wavelength, wedelolactone has adequate absorption according to its three-dimensional ultraviolet absorption spectra. The mean retention time was 4.3±0.1 min, and a chromatogram of standard wedelolactone was presented earlier in Rai and Agrawal (2020).

Statistical analysis

Tukey's HSD test was performed to check the significant difference under intermittent and continuous UV-B treatments compared to ambient UV-B treatment. To examine the effect of treatments (T), growth stage (S), and their interactions (T× S) on *E. alba* plants, a two-way analysis of variance (ANOVA) was tested for various biochemical parameters. The principal component analysis (PCA) was performed to investigate the association pattern among different studied biochemical parameters under IT and CT UV-B treatments at 110 DAG. The dose-effect relationship between treatments of UV-B and wedelolactone concentration was derived through a linear regression curve. All statistical tests were performed using SPSS software (SPSS Inc. version 21.0, IBM Corp, Armonk, NY).

Results

UV-B exposure

The test plants daily received an average of 15.9 kJ m^{-2} ambient UV-B at the experimental plot (Table 1). However, the accumulated UV-B exposure values were 2385, 2697, and 2961 kJ m^{-2} during the entire growth period under ambient, intermittent, and continuous UV-B treatment, respectively (Table 1).

Photosynthetic pigments

The main photosynthetic pigments chlorophyll *a* and chlorophyll *b* varied widely in *E. alba* under IT and CT of UV-B radiation. Chlorophyll *a* content showed a significant increase of 7.26% at 45 DAG under IT. However, significant reductions of 3.44 and 7.06% were observed at 110 DAG under IT and CT, respectively (Fig. 1(a)). A significant decline by 4.9, 19.7, and 25.5% was observed in chlorophyll *b* at 45, 75, and 110 DAG, respectively, under IT, while 6.05, 15.1, and 33.0% reduction were found in CT at 45, 75, and 110 DAG, respectively (Fig. 1(b)). Furthermore, the ratio of chlorophyll *a* and chlorophyll *b* showed a significant increase by 12.8, 23.2, and 28.8% under IT, while 5.8, 18.6, and 36.5% increase were observed under CT at 45, 75, and 110 DAG, respectively (Fig. 1(c)). According to the results of two-way ANOVA, growth stages and eUV-B treatments and their interactions

significantly influenced the chlorophyll *a, b*, and their ratio (Table 2).

The protein content was significantly increased by 1.6 and 2.1% at 45 DAG under IT and CT, respectively (Fig. 1(d)), while a significant decline by 1.3% was recorded under IT at 75 DAG (Fig. 1(d)). Two-way ANOVA results showed that protein content is significantly affected by the growth stages only (Table 2).

Reactive oxygen species and lipid peroxidation

Reactive oxygen species, especially $^{\cdot}O_2^{-}$ production rate, showed a more significant increase at the early stage in both the treatments, and its maximum increase was 122.5% under CT at 45 DAG (Fig. 2(a)). However, plant exposed to IT also showed a significant increase by 80.1, 50.1, and 23.7% at 45, 75, and 110 DAG, respectively (Fig. 2(a)). Two-way ANOVA results showed that the superoxide production rate varied significantly by growth stages, treatments, and interaction (Table 2).

H_2O_2 content was increased significantly by 29.7, 22.7, and 16.4% under IT and 34.1, 47.5, and 27.9% under CT at 45, 75, and 110 DAG, respectively (Fig. 2(b)). The maximum increase in H_2O_2 content was found at 75 DAG under CT (Fig. 2(b)). The H_2O_2 production was significantly affected by the sampling stages and eUV-B treatment as per two-way ANOVA (Table 2).

Lipid peroxidation is estimated by the MDA content in the leaf tissue. The membrane damage under both the treatments were increased significantly by 72, 48.2, and 47.7% under IT and 38.4, 80.5, and 190.2% under CT at 45, 75, and 110 DAG, respectively (Fig. 2(c)). According to the two-way ANOVA results, plant growth stages, treatments, and their interactions significantly affected the lipid peroxidation (Table 2).

The ROS potential was found to be highest under CT compared to IT. The early growth stage (45 DAG) had higher ROS potential for IT; contrary to this, CT had elevated ROS potential at the older stage (110 DAG). Moreover, the ROS potential was 184.6, 121, and 87.7 at 45, 75, and 110 DAG under IT and 194.8, 190.5, and 247.4 at 45, 75, and 110 DAG under CT. In general, the early growth stage is highly susceptible for ROS induction and under both the treatments; hence, more damage was observed (Table 3).

Enzymatic antioxidants

The SOD activity of *E. alba* showed a significant increase at all the growth stages under both treatments. However, the activity was found to be highest at 75 DAG under both treatments (Fig. 3). The catalase activity showed a significant decline by 35.6 and 31.41% at 45 DAG under IT and CT, respectively (Fig. 3). Later, a significant increase by 7.74% was

Table 2 *F*-values and level of significance obtained from two-way ANOVA test

Parameters	Growth stages	Treatment	Growth stages × treatment
Chl *a*	100.52***	76.75***	82.86***
Chl *b*	53.04***	110.61***	53.85***
Chl *a*/Chl *b*	46.82***	166.46***	21.74***
Phenol	2861.4***	226.87***	203.90***
Ascorbic acid	3918.31***	5640.62***	20479.10***
Anthocyanin	587.9***	14.76***	392.63***
Total flavonoids	241.96***	7.28**	163.86***
Proline	1840.16***	766.22***	426.87***
Thiol	813.24***	2411.03***	1555.01***
Protein	48.88***	0.50^{ns}	3.42^{ns}
Tannin	13.71***	3.01^{ns}	1.76^{ns}
Lignin	0.001^{ns}	1.501^{ns}	0.57^{ns}
Superoxide radical production	427.3***	221.05***	25.16**
H_2O_2 content	231.88***	72.72***	3.49^{ns}
LPO	46.42***	316.09***	92.14***
SOD	1288.37***	169.42***	22.49***
APX	247.69***	51.84***	21.59***
CAT	4366.86***	43.84***	167.89***
POX	4672.34***	686.95***	431.79***
GR	1581.71***	4381.99***	903.85***
Total wedelolactone content	201.62***	113.7***	138.49***
Wedelolactone leaf	1055.59***	17.84***	627.93***
Wedelolactone stem	14526.07***	410.33***	892.30***
Wedelolactone root	2362.11***	262.08***	111.7***

***$p < 0.001$; **$p < 0.01$; *$p < 0.05$; *ns* non-significant

observed at 75 DAG under IT, and by 25.24%, and an increase under CT at 75 (Fig. 3). The POD activity was increased significantly by 38.1 and 105.5% under IT at 45 DAG under IT and CT, respectively, and by 14.7% at 75 DAG under CT (Fig. 3). Moreover, a significant decline of 6.2% was observed under IT at the same age (Fig. 3). The APX activity increased significantly at 45 and 75 DAG under both the treatments as compared to AT. The enzyme activity was increased by 11.35 and 24.34% under IT, while 11.29 and 38.66% under CT at 45 and 75 DAG, respectively (Fig. 3). The GR activity was significantly increased by 130.8, 72.2, and 83.3% under IT, and by 38.5, 122.2, and 33.3% under CT was observed at 45, 75, and 110 DAG, respectively (Fig. 3). The SOD, CAT, POD, APX, and GR enzyme activities were significantly influenced by growth stages, eUV-B treatment, and their interactions as per the results of two-way ANOVA (Table 2).

The enzymatic antioxidative potential was found to be highest under CT at 75 DAG, while under IT maximum was observed at 45 DAG. The enzymatic antioxidative potential was 168.4, 129.6, and 82 under IT, and 152.3, 248.4, and 62.6 under CT at 45, 75, and 110 DAG, respectively (Table 3).

Non-enzymatic antioxidants

The most evident effect of both the UV-B exposures on the test plant was observed on total phenolics content, which manifested a significant increase by 13.3 and 16.3% under IT and 32.5 and 36.9% under CT at 45 and 75 DAG, respectively (Fig. 4(a)). Furthermore, at a later stage of growth (110 DAG), a significant decline was observed under both treatments (Fig. 4(a)). The growth stages and eUV-B treatment significantly influenced the total phenolic content and their interactions, as per the two-way ANOVA results (Table 2).

Additionally, ascorbic acid content was significantly increased by 66.5% and 7.7% under IT and 45 and 110 DAG (Fig. 4(b)). In contrast, plants exposed to CT showed a rise in ascorbic acid content only at the initial stage of growth (45 DAG) by 90.5% (Fig. 4(b)). A significant reduction by 6.1% under IT at 75 DAG and 35.8 and 10.5% under CT at 75 and 110 DAG was observed, respectively (Fig. 4(b)). As per two-way ANOVA, the growth stages, treatments, and interactions significantly affected the ascorbic acid content of *E. alba* (Table 2).
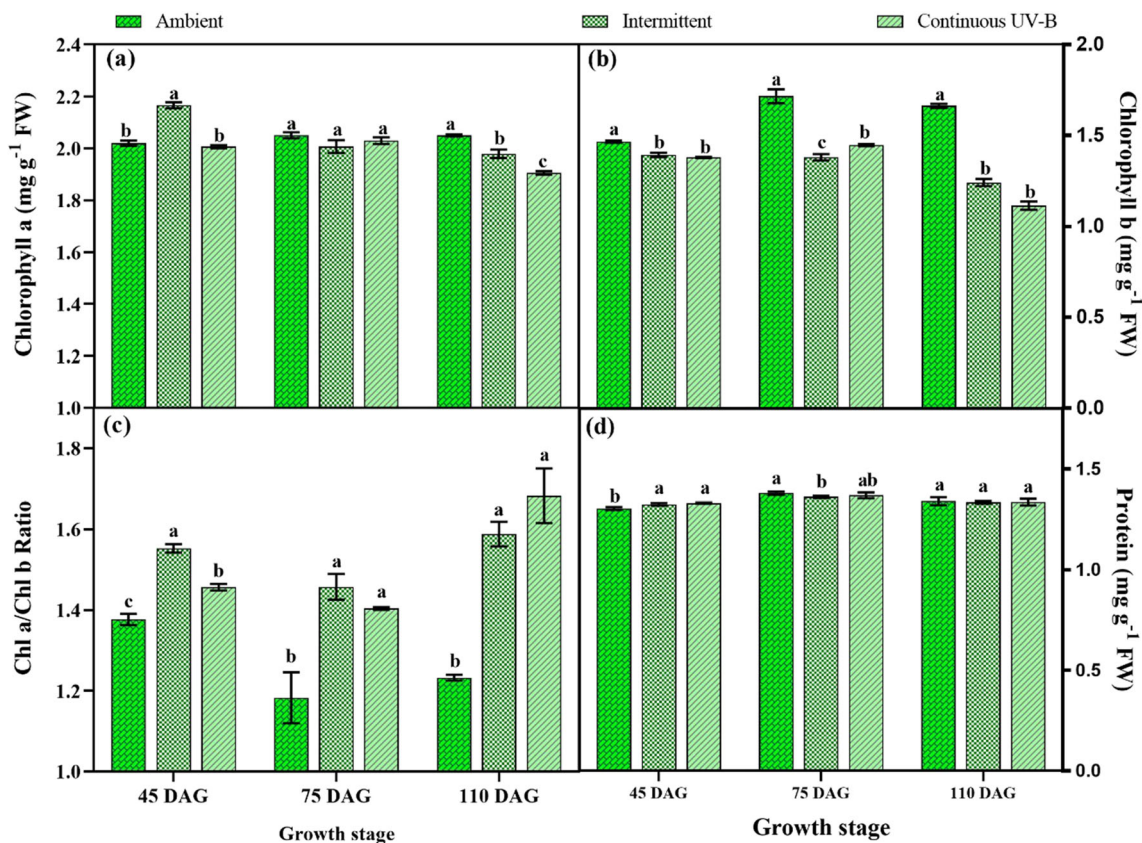
Fig. 1 Chlorophyll *a* (a), chlorophyll *b* (b), chlorophyll a/b ratio (c), and protein content (d) of *E. alba* under ambient, intermittent, and continuous UV-B treatments at three developmental stage. Different letters indicated significant differences between the treatments (mean ± SE, Tukey's HSD, $P < 0.05$, $N = 5$)

Thiol content showed a significant rise by 53.3, and 2.6% under IT at 45 and 75 DAG, while 34.9, 29.3, and 21.8% increase was observed under CT at 45, 75, and 110 DAG, respectively (Fig. 4(c)). However, a reduction by 27.5% was observed under IT at 110 DAG (Fig. 4(c)). Two-way ANOVA results indicated that growth stages, UV-B treatments, and their interactions significantly affected the thiol content (Table 2).

Moreover, a multi-fold rise was observed in proline content at 45 and 75 DAG, but the more significant increase by 435.8% was noted at 45 DAG under CT (Fig. 4(d)). Proline content was significantly affected by growth stages, eUV-B treatment, and their interactions as well (Table 2).

Furthermore, anthocyanin content significantly increased by 42.5% and 30.7% at 45 and 75 DAG under IT, while 79.5% at 45 DAG under CT (Fig. 4(e)). Besides that, a significant decline was observed under IT and CT at 110 DAG (Fig. 4(e)). According to the two-way ANOVA, anthocyanin content was significantly influenced by the test plant's growth stages, treatments, and interactions (Table 2).

UV-B exposure resulted in a significant rise of flavonoids at 45 DAG by 36.5 and 33.9% under IT and CT, respectively (Fig. 4(f)). Significant reductions by 13.6 and 10.3% under IT and 2.7 and 26.8% under CT were noticed at 75 and 110
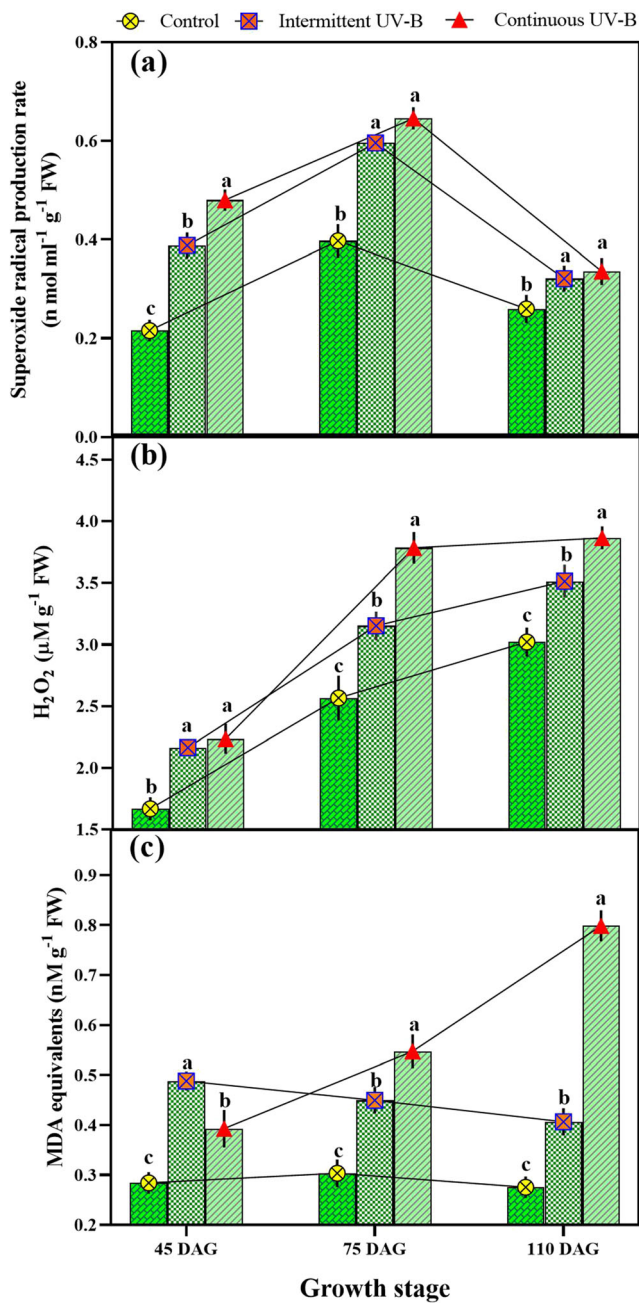
DAG, respectively (Fig. 4(f)). Total flavonoid content was significantly influenced by growth stages and the interactions of growth stages and eUV-B treatments only (Table 2).

Polyphenolic compounds like tannin and lignin showed slight change under both the UV-B treatments. Tannin content showed a significant reduction by 16.2% at 45 DAG under IT (Fig. 4(g)). Tannin content is significantly affected by the plant growth stages only (Table 2). No significant changes were observed in lignin content at all the growth stages due to UV-B treatment, either IT or CT.

Wedelolactone concentration

Among the phytochemical compounds, wedelolactone was individually estimated at all the three growth stages in the leaves, stem, and roots of the test plant. A significant maximum rise in wedelolactone content by 74.5% was observed in leaves at 75 DAG under IT, while an 8.4% increase was observed in CT (Fig. 5(a)). However, a significant decline of 25.7% (110 DAG) under IT and 61.4% and 45.2% at 45 and 110 DAG under CT was also observed in the leaf tissues of *E. alba* (Fig. 5(a)). Additionally, the wedelolactone content estimated in the stem showed a significant decline by 59.4, 60.2, and 26.9% under IT at 45, 75, and 110 DAG,

Fig. 2 Superoxide radical production rate (a), H_2O_2 (b), and MDA content (c) in *E. alba* under ambient, intermittent, and continuous UV-B treatments at three developmental stage. Lines showed the changes with growth stages in each treatment. Different letters indicated significant differences between the treatments (mean ± SE, Tukey's HSD, $P < 0.05$, $N = 5$)

Table 3 Total ROS and enzymatic antioxidative defense potential under intermittent and continuous exposure of UV-B

Growth Stage	ROS potential		Enzyme antioxidative potential	
	IT	CT	IT	CT
45 DAG	184.6	194.8	168.4	152.3
75DAG	121	190.5	129.6	248.4
110 DAG	87.7	247.4	82	62.6

IT intermittent UV-B treatment, *CT* continuous UV-B treatment

DAG under CT (Fig. 5(c)). The wedelolactone content was significantly affected by growth stages, UV-B dose, and their interaction observed in two-way ANOVA results (Table 2). The relationship between UV-B treatment and total wedelolactone concentration (leaf, stem root) was significantly negatively correlated with 0.97 of R^2 at 110 DAG (Fig. 6).
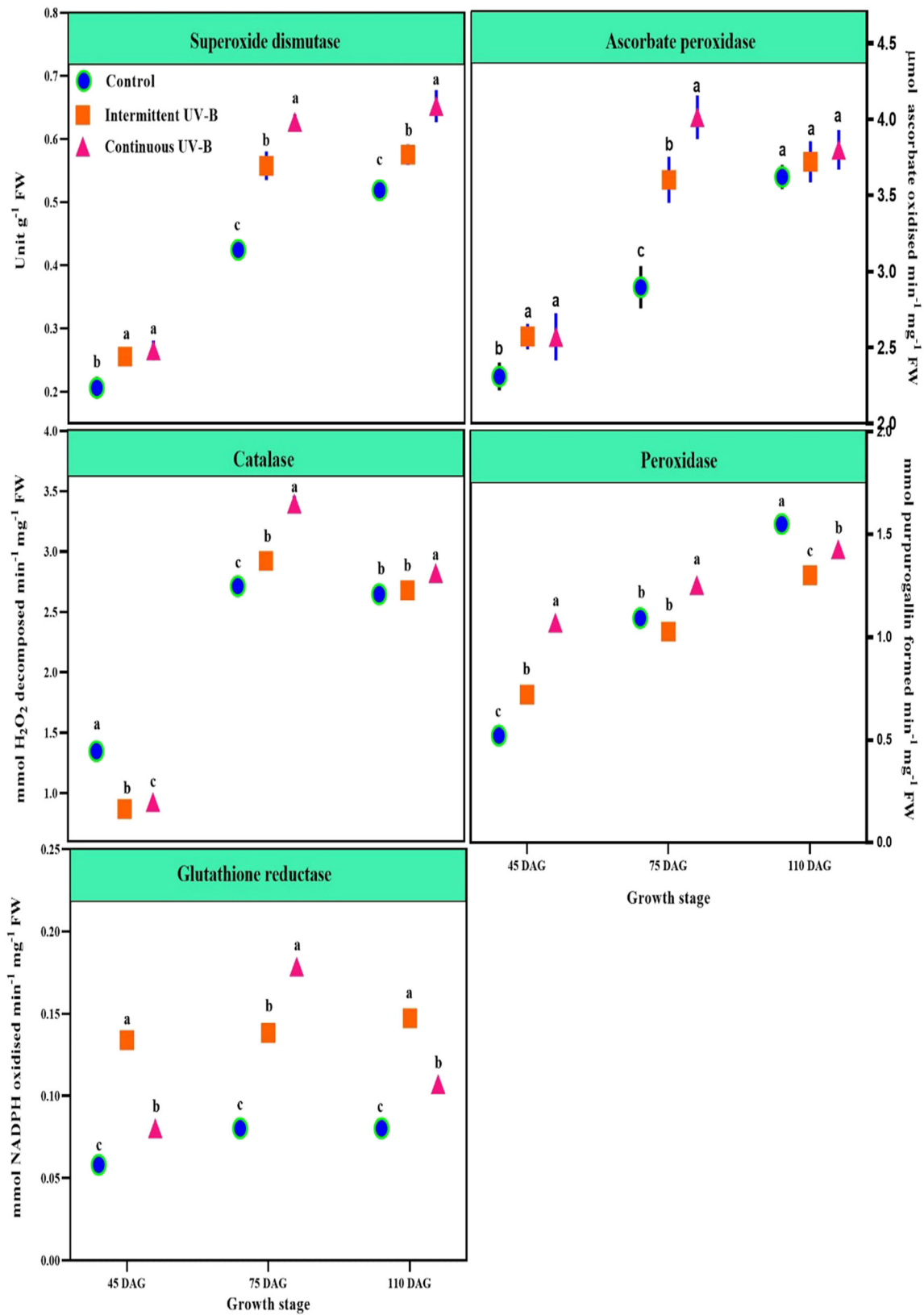
Principle component analysis

PCA analysis showed strong positive associations between intermittent UV-B treatment (IT) and lipid peroxidation, ascorbic acid, GR, and lignin. However, anthocyanin, thiol, POD, flavonoids, chlorophyll *a* and *b*, and wedelolactone were negatively associated with IT at 110 DAG (Fig. 7). For continuous UV-B treatment (CT), H_2O_2 content, lipid peroxidation, O_2^- production, thiol, GR, CAT, SOD, and APX were positively associated. Simultaneously, phenol, flavonoids, wedelolactone, chlorophyll a and chlorophyll b, anthocyanin, ascorbic acid, and POD showed negative associations with CT at 110 DAG (Fig. 7 and Fig. 8).

Discussion

The UV-B-induced accumulation of secondary metabolites is a well-established and known mechanism (Rai and Agrawal 2020; Takshak and Agrawal 2018; Kumari et al. 2009). Here, the impacts of alternate/discontinuous, continuous versus ambient exposure of UV-B on *E. alba* have been studied to find the modulations, if any, and relevance of using two differential UV-B doses. UV-B's deleterious effect is well-documented, but its impact varies with plant species and prevailing environmental factors (Bornman et al. 2019). Variations in the environmental factors such as sunshine hours, temperature fluctuations, and rainfall patterns could be the driving factors; hence, seasonal variations are also essential to monitor under field studies (Coffey et al. 2017).

From the present study's outcome, it is clear that UV-B exposure reduces the chlorophyll pigments, which was also explained by the strong negative correlation of chlorophyll *a* and chlorophyll *b* with IT and CT in the PCA. In agreement

respectively, while recording a 23.6% reduction at 110 DAG under CT (Fig. 5(b)). Apart from that, *E. alba* stem showed a significant increase by 174.8% at 45 DAG under CT compared to AT (Fig. 5(b)). A similar pattern of reduction in wedelolactone content by 49.5 and 11.3% at 45 and 75 DAG under IT and 22.6% at 110 DAG under CT was observed in the roots of *E. alba*, while an increase in wedelolactone content by 79.3% was also observed at 45

Fig. 3 Enzymatic antioxidative defense activities of *E. alba* under ambient, intermittent, and continuous UV-B treatments at three developmental stage. Different letters indicated significant differences between the treatments (mean ± SE, Tukey's HSD, *P* < 0.05, *N* = 5)
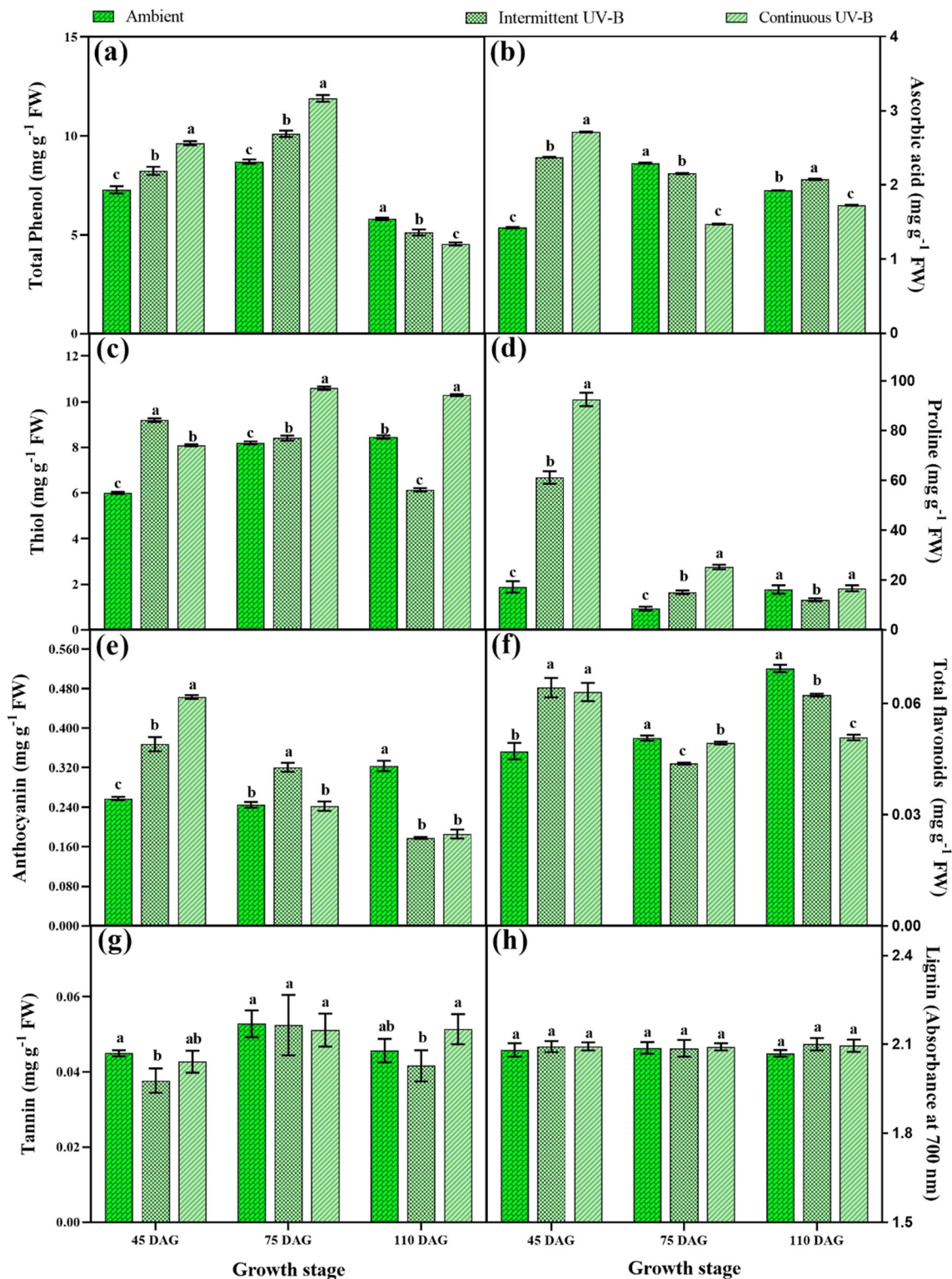
Fig. 4 Total phenolic (a), ascorbic acid (b), thiol (c), and proline content (d), anthocyanin (e), total flavonoids (f), tannin (g), and lignin (h) of *E. alba* under ambient, intermittent, and continuous UV-B treatments at 45, 75, and 110 days after germination. Different letters indicated significant differences between the treatments (mean ± SE, Tukey's HSD, $P < 0.05$, $N = 5$)

with our results, Salama et al. (2011) have also reported a decline in the chlorophyll *a* and *b* in *Malva parviflora* L., *Plantago major* L., *Rumex vesicarius* L., and *Sismbrium*

erysimoids Desf. They also suggested the sensitivity of photosynthetic pigment varies from species to species, and chlorophyll *a* could be subjected to more selective
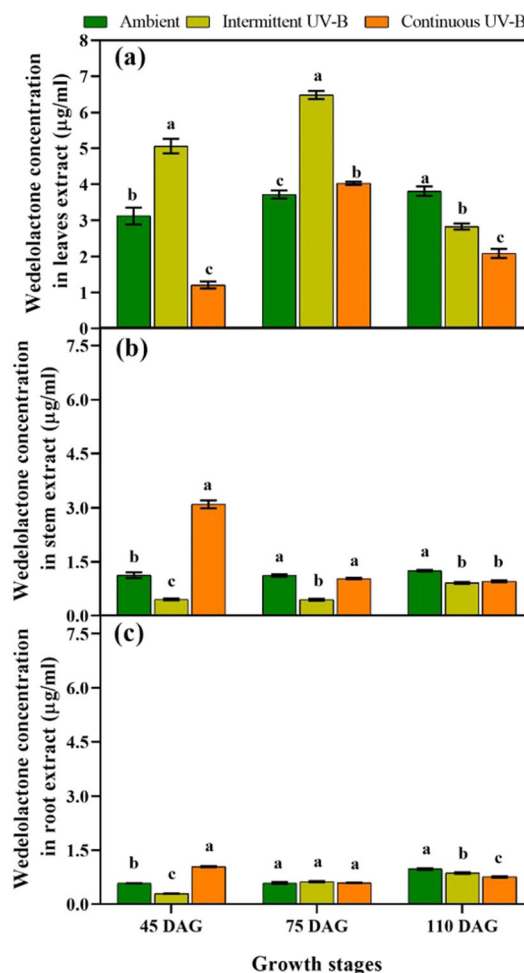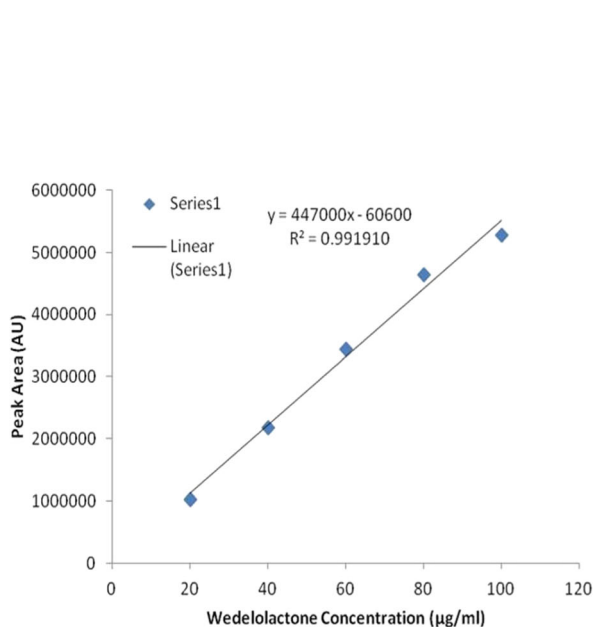
Fig. 5 Wedelolactone concentration in different parts (leaf (a), stem (b), and root (c)) of *E. alba* at 45, 75, and 110 DAG growth stages under ambient, intermittent, and continuous UV-B treatments. Different letters indicated significant differences between the treatments (mean ± SE, Tukey's HSD, $P < 0.05$, $N = 3$)

degradation compared to chlorophyll *b*. Hamid et al. (2019) have also reported the degradation of photosynthetic pigments due to thylakoid damage induced by enhanced ROS, driven
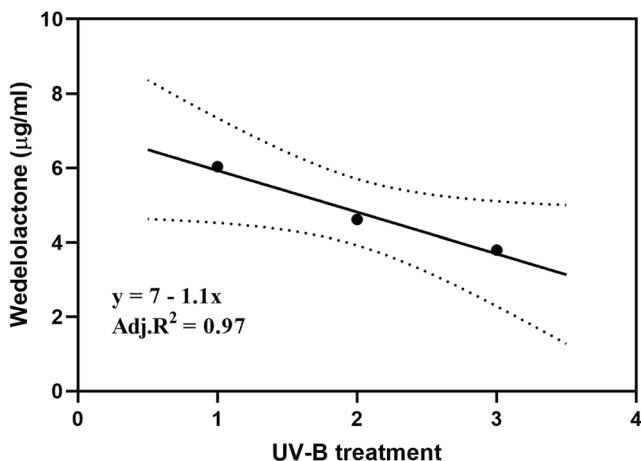
Fig. 6 Linear regression between the three UV-B treatments and wedelolactone concentrations of *E. alba* at the final growth stage (110 DAG). The dashed line indicates the 95% confidence interval

from eUV-B exposure in *Heteropogon contortus*. However, a slight increase in chlorophyll *a* content at the initial growth stage under IT could be due to the hormetic effect shown by the *E. alba* in response to IT and involved recovery period. The increase in the ratio of chlorophyll *a/b* facilitates the adaptation of the test plant against oxidative stress by maximizing the energy efficiency and allowing it to maintain efficient and stable photosynthetic processes. This implies that the test plant's oxidative stress response machinery under both the eUV-B treatments spends too much energy for oxidative defense (Reyes-Díaz et al. 2016). The variable results of the protein content of *E. alba* might be due to the synthesis of various UV-protective compounds. The increase in protein content was also reported in *H. contortus* BL-1 under elevated UV-B (ambient±7.2 kJ m^{-2} day^{-1}) (Hamid et al. 2019). The aggravation in photosynthetic pigments and acceleration of protein content under eUV-B exposure suggested the imbalance in the production and scavenging of ROS, thus, creating photo-oxidative damage to the plant.
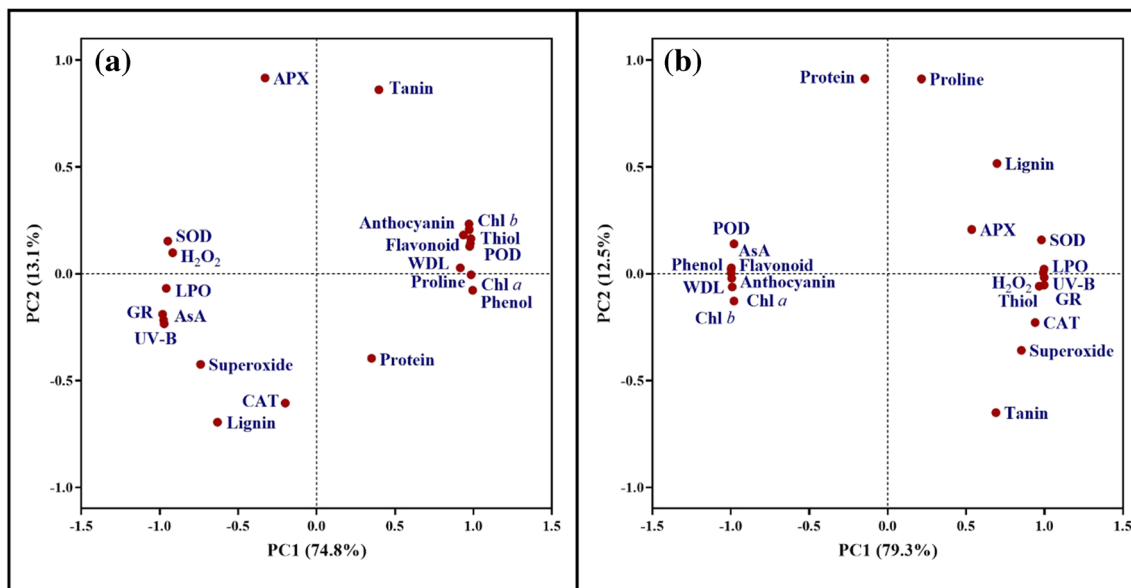
Fig. 7 Principal component analysis biplot representing two principal components (PC1 and PC2) axis explaining 74.8 and 13.1% variance for intermittent UV-B treatment (**a**) and 79.3 and 12.5% of total variance for continuous UV-B treatment (**b**) at 110 DAG. APX: ascorbate peroxidase, AsA: ascorbic acid content, CAT: catalase, GR: glutathione reductase, H_2O_2: hydrogen peroxide production rate, LPO: lipid peroxidation, POD: peroxidase, superoxide: superoxide radical production; SOD: superoxide dismutase, UV-B: UV-B treatment, WDL: wedelolactone

Among ROS, the superoxide radical ($\cdot O_2^-$) production and H_2O_2 content found to be increased under both treatments. However, ROS production was found higher in CT when compared to AT. PCA exhibits a strong positive correlation of H_2O_2 than $\cdot O_2^-$ with CT exposure, this higher H_2O_2 compared to $\cdot O_2^-$ probably due to higher superoxide dismutase

(SOD) scavenging activity, which decomposes the $\cdot O_2^-$ to produce non-toxic H_2O_2 and O_2. Furthermore, the H_2O_2 content, $\cdot O_2^-$, and SOD activity were found to be higher in CT than in IT against AT. The increased malondialdehyde content (MDA) is associated with photo-oxidative damage induced by the enhanced lipid peroxidation of the cellular and organellar

Fig. 8 Morphological alterations (**a**), visible leaf injuries (**b**), and anatomical changes (**c**) induced by intermittent and continuous UV-B radiation in *E. alba* as compared to ambient
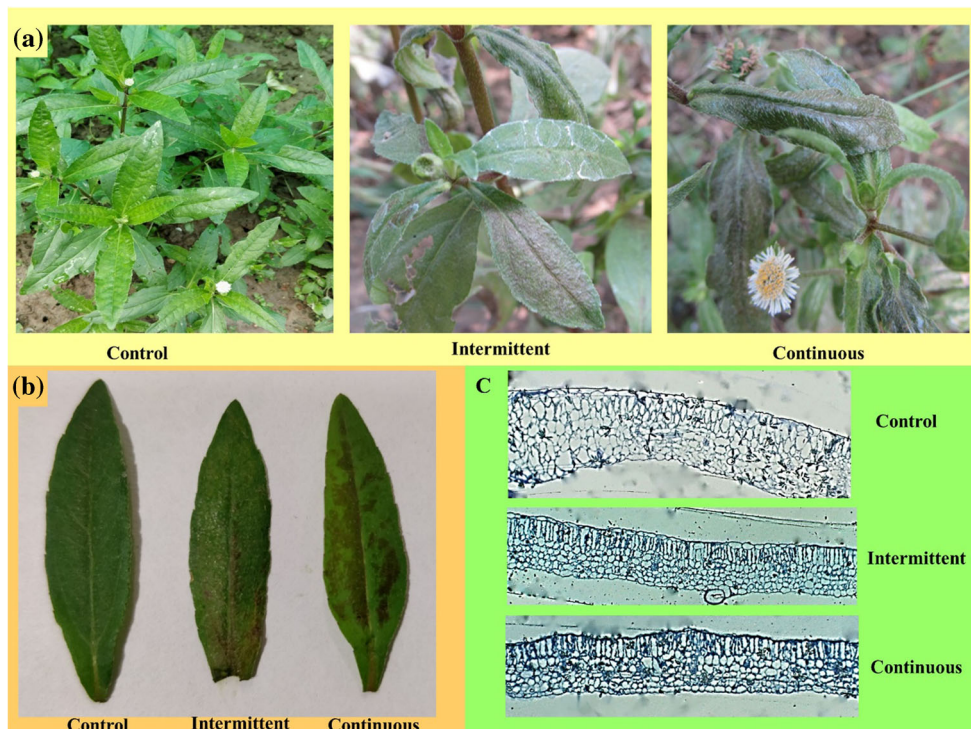
membrane and was observed in this study. Initially, the membrane damage under IT was more as compared to that under CT. But at later stages, membrane damage was found significantly higher under CT, which was also in agreement with PCA results. This enhanced membrane damage could be correlated to the oxidative stress induced by an imbalance in H_2O_2 and $^{.}O_2^{-}$ production (including other ROS, too) (Takshak and Agrawal 2018).

The SOD activity neutralizes $^{.}O_2^{-}$ via its dismutation, and H_2O_2 content in the plant has been scavenged by the catalase (CAT), several peroxidases (POD), and ascorbate-glutathione (ASH-GSH)-related enzymes. H_2O_2 is the most occurring and abundant ROS, which regulates most of the reactions involving ROS. CAT converts H_2O_2 into H_2O and O_2; hence, it is one of the most important antioxidative enzymes. However, the CAT activity was lower at the initial growth stage, but later with increment in stress-induced production of H_2O_2 content in the stressed plant, CAT also showed stimulation in enzyme activity. An increase in CAT activity was also reported in *H. contortus* (Hamid et al. 2019), *Coleus forskohlii*, *Withania somnifera* (Takshak and Agrawal 2014a, b, 2015), and *Helianthus annuus* (Hagh et al. 2012) and in agreement with our results. The ascorbate peroxidase (APX) also played a crucial role in H_2O_2 scavenging and maintaining the cells' redox potential under prevailing stress. In the present experiment, the APX activity showed augmentation with UV-B treatment and was found to be highest at 75 DAG under CT. Our results corroborate with the increased APX activity reported in *H. contortus*, *C. forskohlii*, *W. somnifera*, and *H. annuus* (Hamid et al. 2018; Takshak and Agrawal 2014a, b, 2015; Hagh et al. 2012). The peroxidase activity (POD) also helps decompose H_2O_2 via the co-substrate oxidation, and an increase in POD activity under eUV-B has been reported by Takshak and Agrawal (2014a, b) in *W. somnifera*. In our experiment, the POD showed augmented activities up to 75 DAG (up to maturity) but showed a reduction at senescence (110 DAG). It is therefore conclusive to say, the senescence stage pertains to the declining efficiency of POD enzymes in combating oxidative stress. In the present study, the GR activity was found to be higher under IT at the initial and final growth stages. Moreover, GR activity at 75 DAG was higher under CT. The GR activities' fluctuations at different growth stages are indicative of the reduced efficiency of the ASH-GSH cycle at 45 and 110 DAG in the test plant exposed under CT and are also weaker to decompose the enhanced ROS efficiently. Similar results were observed in *H. contortus* under eUV-B treatment (ambient±7.2 kJ m^{-2} day^{-1}) (Hamid et al. 2019). PCA displayed that CT exposure positively influenced all the tested antioxidative enzymes except POD at 110 DAG because it reduces increased ROS level.

ROS potential describes the damaging extent of the overall ROS produced in response to eUV-B exposure. In the present study, it was found to be higher at initial growth stages under both treatments. However, under IT, the recovery time helped the test plant to acclimatize against the prevailing stress, ultimately reducing the ROS potential. Furthermore, in the case of CT, the long and continuous UV-B exposure led to increased ROS potential indicating the enhanced oxidative response costing the overall plant performances.

Moreover, the enzymatic antioxidative potential showed the test plant's overall antioxidative response in response to the prevailing stress. This study found that the enzymatic response against the enhanced stress was also very strong at initial growth stages and continues up to 75 DAG. Later, at 110 DAG, the enzymatic antioxidative potential of IT reaches approximately equal to ROS potential to create a balance between the stress and response. But the enzymatic antioxidative potential of CT declines due to lack of recovery period, and it gets weaker at senescence, leading to an increase in ROS potential.

The eUV-B is known for inducing the enhanced secondary metabolites' biosynthesis and accumulation. In this study, an increase in phenolic content under IT and CT was observed up to 75 DAG. The phenolic content screen-out most of the harmful UV-B radiation by accumulating at the surface or acting as a screening agent. It also plays a regulatory role in combating oxidative stress via its antioxidative properties (Sharma et al. 2019; Król et al. 2014). The phenylpropanoid pathway–derived compounds, including various phenolic, phenolic acids, flavonoids, coumarins, stilbenes, and lignans, have multiple structural integrity roles, as screening pigments, signaling, and defense (Sharma et al. 2019; Takshak and Agrawal 2016; Król et al. 2014; Douglas 1996). The present results showed a decline in phenolic content at later stages of the test plant's growth, which indicates that at the senescence stage, the photosynthates are more involved in the biosynthesis of phenolic compounds.

Flavonoids are the most common polyphenolic compounds involved in the photoprotection of plants from bright light. Its potential antioxidative properties help in screening UV-B radiation in plants. In the present study, an increase in flavonoid content was observed with increasing eUV-B doses to protect against UV damage and help the plants acclimatize and adapt under prevailing stress. Various studies have reported increased flavonoid content in plants under enhanced UV-B (Sharma et al. 2019; Takshak and Agrawal 2018; Rai and Agrawal 2017). Later, reduction in flavonoid content corroborates the decrease of phenolic content in the test plant's senescence stages. This might be due to photosynthates' allocation towards terpenes biosynthesis (essential oil content earlier presented in Rai and Agrawal 2020). Król et al. (2014) suggested that short-term stress exposure of UV-B enhances the phenolic compounds (including phenolic acids and flavonoids), but the long-term stress exposure-response mechanism is different, and it varies with the type of stress, its intensity, its duration, growth, and developmental stages of the plants and plant

tissues. Hence, a slowdown in a selected secondary metabolite's biosynthesis can reduce the energy expenditure and could be a strategy for survival in unfavorable conditions.

Other important polyphenolic compounds synthesized as the end-product of phenylpropanoid pathways are lignin and tannins; they are also involved in the protection of the plants under stress. Lignins are a structural component of some cells' plant cell walls, which are involved in imparting mechanical strength and water impermeability to the plants (Douglas 1996). In the present study, lignin content was not affected by both the UV-B treatments; this might be the herbaceous nature of the test plant. However, tannins are high molecular weight polyphenolic compounds stored into tannosomes (a chlorophyllous organelle enclosed within the tonoplast) (Sieniawska and Baj 2017). An increase in tannin content is mostly related to protection against the insect, microbial, or animal infection/attack and is also involved in ROS detoxification and inhibits lipid peroxidation (Sieniawska and Baj 2017). Tannin content showed negative alteration under IT, which depicts UV-B-induced disturbances into the tannins' structure and damage to their storage region (chlorophyllous tannin). Moreover, Harding (2019) suggested the flavonoid biosynthetic pathway derived from the synthesis of tannins; their lower accumulation could indicate a metabolic modification in its biosynthesis in high humid conditions (Top et al. 2017). Glutathione is found either in GSSG (free, oxidized) form or in GSH (bound, reduced) form and is involved in detoxification of ROS along with ascorbate peroxidase via Halliwell-Asada pathway. It plays a crucial role in the regeneration of ascorbic acid in the pathway to yield GSSG. An increase in thiol content in *E. alba* up to 75 DAG under IT and up to110 DAG under CT corroborates with the studies on *C. forskohlii* (Takshak and Agrawal 2015), *Cimbopogon citratus*, and *A. calamus* (Kumari et al. 2009, 2010), which is a counteraction of the test plant against peroxidation-linked damages.

The non-enzymatic arrays for mitigating ROS toxicity were assessed via proline and ascorbic acid estimations. Proline is an amino acid involved in ROS detoxification, and an increase in proline content under enhanced UV-B exposure has also been shown in various studies (Takshak and Agrawal 2015; Kumari et al. 2009, 2010). A similar pattern of increase in proline content was recorded in the present study up to 75 DAG, and enhancement in proline content might support its protective role against UV-B stress (Dwivedi et al. 2015).

Ascorbic acid is a key substrate involved in ROS decomposition either because of its regenerative properties or via amplification of its biosynthesis. An increase in ascorbic acid content has been reported in *W. somnifera* and *C. forshkohlii* (Takshak and Agrawal 2014a, b, 2015). The decline in ascorbic acid content is due to a higher UV-B dose for a longer time, coinciding with the PCA result. Khan et al. (2012) also suggested that UV radiation enhances ascorbic acid degradation at higher doses, and this reaction gets augmented with increasing exposure time.

Enhancement in anthocyanin biosynthesis is a counteracting response of the test plant against eUV-B (Takshak and Agrawal 2015). It is also a UV screening compound, and usually gets accumulated in the epidermal cell surfaces to filter the incoming harmful radiations, and it also helps in combating oxidative stress. However, reducing anthocyanin content might be due to the biosynthetic pathway's impairment or degradation of the precursors.

Wedelolactone, coumarin-derived coumestans, is the major compound found in *E. alba*, synthesized via phenylpropanoid pathway (Luo et al. 2018). The studies related to the tissue-specific extraction of wedelolactone (Shailajan et al. 2016) are very few, which can validate the alterations in wedelolactone concentration under eUV-B. So, this study confirms the presence of significant alterations induced by both the treatment of eUV-B on wedelolactone content in leaves, stem, and roots. In the present study, the increase in phenolic content at the test plant's initial growth stages corroborates the biosynthesis of wedelolactone in different tissues. Under IT exposure at 75 DAG, the wedelolactone content showed maximum biosynthesis in the plant's leaf tissues (wedelolactone data observed at 75 DAG were earlier presented in Rai and Agrawal 2020). However, in shoot and root tissues, the wedelolactone content was found to be higher under CT, which indicates that initial growth stages are the best time for the extraction of wedelolactone content from *E. alba*. PCA exhibit a strong negative correlation of wedelolactone with UV-B exposure at 110 DAG. The reduction of wedelolactone in all three tissues at 110 DAG might be due to the destruction of its precursors under long exposure to UV-B.

Conclusions

From the present study, it can be concluded that both IT (~130 h) and CT (~240 h) eUV-B exposure compromises plant performance and alter the expression of the metabolites found in the test plant. Each plant performs differentially to alternate/discontinuous stress compared to prolonged continuous stresses, and it is also not necessary that their response results in growth penalties. But in this study, the antioxidative compounds from the CT-exposed plants become more potent in ROS detoxification, which on the one hand indicates the adaptation strategies of the plant against oxidative stress and, on the other hand, also showed the maximum allocation of assimilates towards defense. This assimilates allocation trade-off costs the wedelolactone biosynthesis in CT as compared to IT. However, our study is the first dose-dependent response estimation attempt to determine the alterations in wedelolactone content under two different UV-B doses.

Higher content of wedelolactone can be exploited from the leaves exposed to IT of UV-B at the early growth stage of *E. alba*. Further studies on animal models are required to optimize the pharma- and nutraceutical efficiency of wedelolactone and other medicinally important compounds of *E. alba* under different doses of UV-B.

Author contribution K. R. collected, estimated, analyzed, and interpreted the experimental data. S. B. A. planned the experiment, and checked and evaluated the data and manuscript. All authors read and approved the final manuscript.

Availability of data and materials Not applicable

Declarations

Ethical approval Not applicable

Consent to participate Not applicable

Consent to publish Not applicable

Competing interests The authors declare no competing interests.

References

Alexieva V, Sergiev I, Mapelli S, Karanov E (2001) The effect of drought and ultraviolet radiation on growth and stress markers in pea and wheat. Plant Cell Environ 24(12):1337–1344. https://doi.org/10.1046/j.1365-3040.2001.00778.x

Bates LS, Waldren RP, Teare ID (1973) Rapid determination of free proline for water-stress studies. Plant Soil 39(1):205–207.

Beyer WF, Fridovich I (1987) Assaying for superoxide dismutase activity: Some large consequences of minor changes in conditions. Anal Biochem 161(2):559–566. https://doi.org/10.1016/0003-2697(87)90489-1

Bornman JF, Barnes PW, Robson TM, Robinson SA, Jansen MAK, Ballare CL, Flint SD (2019) Linkages between stratospheric ozone, UV radiation and climate change and their implications for terrestrial ecosystems. Photochem Photobiol Sci 18(3):681–716. https://doi.org/10.1039/c8pp90061b

Bradford MM (1976) A rapid and sensitive method for the quantitation of microgram quantities of protein utilizing the principle of protein-dye binding. Anal Biochem 72(1-2):248–254

Bray HG, Thorpe WV (1954) Analysis of phenolic compounds of interest in metabolism. Methods Biochem Anal 1:27–52

Britton C, Maehly AC (1955) Assay of catalase and peroxidase. In: Colowick, S.P., Kaplan, N.O., (ed.) Academic Press, New York. Methods in Enzymol 2:764–775

Chang CC, Yang MH, Wen HM, Chern JC (2002) Estimation of total flavonoid content in propolis by two complementary colometric methods. J Food Drug Anal 10(3):178–182

Coffey A, Prinsen E, Jansen MAK, Conway J (2017) The UVB photoreceptor UVR8 mediates accumulation of UV-absorbing pigments, but not changes in plant morphology, under outdoor conditions. Plant Cell Environ 40(10):2250–2260. https://doi.org/10.1111/pce.13025

Dai Q, Shaobing P, Chavez AQ, Vergara BS (1994) Intraspecific responses of 188 rice cultivars to enhanced UVB radiation. Environ Exp Bot 34(4):433–442. https://doi.org/10.1016/0098-8472(94)90026-4

Dalton DA, Russell SA, Hanus FJ, Pascoe GA, Evans HJ (1986) Enzymatic reactions of ascorbate and glutathione that prevent peroxide damage in soybean root nodules. Proc Natl Acad Sci 83(11):3811–3815. https://doi.org/10.1073/pnas.83.11.3811

Deikman J, Hammer PE (1995) Induction of anthocyanin accumulation by cytokinins in Arabidopsis thaliana. Plant Physiol 108(1):47–57

Douglas CJ (1996) Phenylpropanoid metabolism and lignin biosynthesis: from weeds to trees. Trends Plant Sci 1(6):171–178. https://doi.org/10.1016/1360-1385(96)10019-4

Dwivedi R, Singh VP, Kumar J, Prasad SM (2015) Differential physiological and biochemical responses of two Vigna species under enhanced UV-B radiation. J Radiat Res Appl Sci 8(2):173–181. https://doi.org/10.1016/j.jrras.2014.12.002

Elstner EF, Heupel A (1976) Inhibition of nitrite formation from hydroxylammoniumchloride: a simple assay for superoxide dismutase. Anal Biochem 70(2):616–620. https://doi.org/10.1016/0003-2697(76)90488-7

Fahey RC, Brown WC, Adams WB, Worsham MB (1978) Occurrence of glutathione in bacteria. J Bacteriol 133(3):1126–1129. https://doi.org/10.1128/jb.133.3.1126-1129.1978

Gitelson AA, Merzlyak MN, Chivkunova OB (2001) Optical properties and nondestructive estimation of anthocyanin content in plant leaves¶. Photochem Photobiol 74(1):38–45. https://doi.org/10.1562/0031-8655(2001)074<0038:opaneo>2.0.co;2

Hagh AG, Khara J, Darvishzadeh R (2012) Effect of UV-B radiation on activity of antioxidant enzymes in four sunflower cultivars. Int J Agric: Res Rev 2(5):528–534

Hamid A, Singh S, Agrawal M, Agrawal SB (2019) Heteropogon contortus BL-1 (Pilli Grass) and elevated UV-B radiation: the role of growth, physiological, and biochemical traits in determining forage productivity and quality. Photochem Photobiol 95(2):572–580. https://doi.org/10.1111/php.12990

Harding SA (2019) Condensed tannins: arbiters of abiotic stress tolerance? Tree Physiol 39(3):341–344. https://doi.org/10.1093/treephys/tpz005

Heath RL, Packer L (1968) Photoperoxidation in isolated chloroplasts. Arch Biochem Biophys 125(1):189–198. https://doi.org/10.1016/0003-9861(68)90654-1

Höll J, Lindner S, Walter H, Joshi D, Poschet G, Pfleger S, Ziegler T, Hell R, Bogs J, Rausch T (2019) Impact of pulsed UV-B stress exposure on plant performance: how recovery periods stimulate secondary metabolism while reducing adaptive growth attenuation. Plant Cell Environ 42(3):801–814. https://doi.org/10.1111/pce.13409

Hossain MA, Asada K (1984) Inactivation of ascorbate peroxidase in spinach chloroplasts on dark addition of hydrogen peroxide: its protection by ascorbate. Plant Cell Physiol 25(7):1285–1295. https://doi.org/10.1093/oxfordjournals.pcp.a076837

Kataria S, Jajoo A, Guruprasad KN (2014) Impact of increasing ultraviolet-B (UV-B) radiation on photosynthetic processes. J

Photochem Photobiol B Biol 137:55–66. https://doi.org/10.1016/j.jphotobiol.2014.02.004

Keller T, Schwager H (1977) Air pollution and ascorbic acid. Eur J For Pathol 7(6):338–350. https://doi.org/10.1111/j.1439-0329.1977.tb00603.x

Khan T, Mazid M, Mohammad F (2012) A review of ascorbic acid potentialities against oxidative stress induced in plants. J Agrobiol 28(2):97–111. https://doi.org/10.2478/v10146-011-0011-x

Khomdram SD, Singh PK (2011) Polyphenolic compounds and free radical scavenging activity in eight Lamiaceae herbs of Manipur. Notulae Sci Biologicae 3(2):108–113

Król A, Amarowicz R, Weidner S (2014) Changes in the composition of phenolic compounds and antioxidant properties of grapevine roots and leaves (vitis viniferal.) under continuous of long-term drought stress. Acta Physiol Plant 36(6):1491–1499. https://doi.org/10.1007/s11738-014-1526-8

Kumar S, Dhanani T (2013) Development and validation of a rapid high performance liquid chromatography – photodiode array detection method for estimation of a bioactive compound wedelolactone in extracts of Eclipta alba. Braz J Pharm Sci 49(1):57–63

Kumari R, Singh S, Agrawal SB (2009) Combined effects of Psoralens and ultraviolet-B on growth, pigmentation and biochemical parameters of Abelmoschus esculentus L. Ecotoxicol Environ Saf 72(4):1129–1136. https://doi.org/10.1016/j.ecoenv.2008.12.009

Kumari R, Singh S, Agrawal SB (2010) Response of ultraviolet-B induced antioxidant defense system in a medicinal plant. Acorus calamus. J Environ Biol 31(6):907–911

Luo Q, Ding J, Zhu L, Chen F, Xu L (2018) Hepatoprotective effect of wedelolactone against concanavalin A-induced liver injury in mice. Am J Chin Med 46(04):819–833

Mosadegh H, Trivellini A, Ferrante A, Lucchesini M, Vernieri P, Mensuali A (2018) Applications of UV-B lighting to enhance phenolic accumulation of sweet basil. Sci Hortic 229:107–116. https://doi.org/10.1016/j.scienta.2017.10.043

Rai K, Agrawal SB (2017) Effects of Uv-B radiation on morphological, physiological and biochemical aspects of plants : an overview. In: J Sci Res 61:75–101

Rai K, Agrawal SB (2020) Effect on essential oil components and wedelolactone content of a medicinal plant Eclipta alba due to modifications in the growth and morphology under different exposures of ultraviolet-B. Physiol Mol Biol Plants 26(4):773–792. https://doi.org/10.1007/s12298-020-00780-8

Reyes-Díaz M, Meriño-Gergichevich C, Inostroza-Blancheteau C, Latsague M, Acevedo P, Alberdi M (2016) Anatomical, physiological, and biochemical traits involved in the UV-B radiation response in highbush blueberry. Biol Plant 60(2):355–366. https://doi.org/10.1007/s10535-015-0580-4

Rubio MC, González EM, Minchin FR, Webb KJ, Arrese-Igor C, Ramos J, Becana M (2002) Effects of water stress on antioxidant enzymes of leaves and nodules of transgenic alfalfa overexpressing superoxide dismutases. Physiol Plant 115(4):531–540. https://doi.org/10.1034/j.1399-3054.2002.1150407.x

Salama HMH, Al Watban AA, Al-Fughom AT (2011) Effect of ultraviolet radiation on chlorophyll, carotenoid, protein and proline contents of some annual desert plants. Saudi J Biol Sci 18(1):79–86. https://doi.org/10.1016/j.sjbs.2010.10.002

Sebastian A, Kumari R, Kiran BR, Prasad MNV (2018) Ultraviolet B induced bioactive changes of enzymatic and non-enzymatic antioxidants and lipids in Trigonella foenum-graecum L.(Fenugreek). The Euro Biotech J 2(1):64–71

Shailajan S, Menon S, Singh D, Swar G (2016) Validated analytical RP-HPLC method for quantitation of wedelolactone from Eclipta alba and marketed Ayurvedic formulations. Pharm J 8(2):132–139. https://doi.org/10.5530/pj.2016.2.6

Sharma A, Shahzad B, Rehman A, Bhardwaj R, Landi M, Zheng B (2019) Response of phenylpropanoid pathway and the role of polyphenols in plants under abiotic stress. Molecules 24(13):2452

Sieniawska E, Baj T (2017) Tannins. In: Pharmacognosy: Fundamentals, Applications and Strategy. Elsevier: Amsterdam, The Netherlands 199–232. https://doi.org/10.1016/B978-0-12-802104-0.00010-X

Syros T, Yupsanis T, Zafiriadis H, Economou A (2004) Activity and isoforms of peroxidases, lignin and anatomy, during adventitious rooting in cuttings of Ebenus cretica L. J Plant Physiol 161(1):69–77

Takshak S, Agrawal SB (2014a) Effect of ultraviolet-B radiation on biomass production, lipid peroxidation, reactive oxygen species, and antioxidants in Withania somnifera. Biol Plant 58(2):328–334. https://doi.org/10.1007/s10535-014-0390-0

Takshak S, Agrawal SB (2014b) Secondary metabolites and phenylpropanoid pathway enzymes as influenced under supplemental ultraviolet-B radiation in Withania somnifera Dunal, an indigenous medicinal plant. J Photochem Photobiol B Biol 140:332–343. https://doi.org/10.1016/j.jphotobiol.2014.08.011

Takshak S, Agrawal SB (2015) Defence strategies adopted by the medicinal plant Coleus forskohlii against supplemental ultraviolet-B radiation: augmentation of secondary metabolites and antioxidants. Plant Physiol Biochem 97:124–138. https://doi.org/10.1016/j.plaphy.2015.09.018

Takshak S, Agrawal SB (2016) Ultraviolet-B irradiation : a potent elicitor of phenylpropanoid pathway compounds. J Sci Res 60(January):79–96

Takshak S, Agrawal SB (2018) Interactive effects of supplemental ultraviolet-B radiation and indole-3-acetic acid on Coleus forskohlii Briq.: alterations in morphological-, physiological-, and biochemical characteristics and essential oil content. Ecotoxicol Environ Saf 147(August 2017):313–326. https://doi.org/10.1016/j.ecoenv.2017.08.059

Takshak S, Agrawal SB (2019) Defense potential of secondary metabolites in medicinal plants under UV-B stress. J Photochem Photobiol B Biol 193:51–88. https://doi.org/10.1016/j.jphotobiol.2019.02.002

Top SM, Preston CM, Dukes JS, Tharayil N (2017) Climate influences the content and chemical composition of foliar tannins in green and senesced tissues of Quercus rubra. Front Plant Sci 8(May). https://doi.org/10.3389/fpls.2017.00423

Tripathi R, Sarkar A, Pandey Rai S, Agrawal SB (2011) Supplemental ultraviolet-B and ozone: Impact on antioxidants, proteome and genome of linseed (Linum usitatissimum L. cv. Padmini). Plant Biol 13(1):93–104. https://doi.org/10.1111/j.1438-8677.2010.00323.x